EurJIC European Journal of Inorganic Chemistry

FULL PAPER

DOI: 10.1002/ejic.201200681

Water-Soluble (Pterin)rhenium(I) Complex: Synthesis, Structural Characterization, and Two Reversible Protonation–Deprotonation Behavior in Aqueous Solutions

Fabricio Ragone,[a] Gustavo T. Ruiz,*[a] Oscar E. Piro,[b] Gustavo A. Echeverría,[b] Franco M. Cabrerizo,[c] Gabriela Petroselli,[d] Rosa Erra-Balsells,[d] Kenzo Hiraoka,[e] Fernando S. García Einschlag,[a] and Ezequiel Wolcan*[a]

Keywords: Rhenium / N,O ligands / Acidity / Pterin

A new water-soluble complex, $Re(CO)_3$(pterin)(H_2O), was synthesized and characterized by ^1H NMR and FTIR spectroscopy, and by a combination of three mass spectrometry techniques: MALDI, probe electrospray ionisation (PESI), and ESI. Because, unlike most metal-pterin complexes, the Re^I complex is quite soluble in water, appropriate single crystals could be obtained for structural X-ray analysis. We report here the first solid state molecular structure containing a pterin ligand coordinated to the $Re(CO)_3$ core. This determination revealed that strong H bonds between the hydrogen atom of the 2-amino group and crystallization water molecules give rise to a polymeric arrangement of $Re(CO)_3$(pterin)(H_2O) complexes in the lattice. Protonation studies in aqueous solutions of the Re^I complex showed two acid-base equilibriums with pK_{a1} = 3.9 and pK_{a2} = 8.8. pK_{a1} was assigned to the protonation equilibrium at N3 of the pterin ligand in the complex and pK_{a2} could be ascribed to the deprotonation of a coordinated water molecule.

Introduction

The interest in the study of organometallic compounds is due to their catalytic properties in synthetic reactions and their role in relevant biological processes. Complexes of the type $XRe(CO)_3L$ are of continuous interest due to their applicability in broad research areas such as electron transfer studies,[1] solar energy conversion,[2] and catalysis.[3] Possible applications as luminescent sensors,[4] molecular materials for nonlinear optics[5] or optical switching[6] have also emerged. In particular, luminescent transition metal complexes of Re^I and Ru^{II} with polypyridyl ligands have been recognized as good potential candidates for the development of pH sensing devices.[7] Moreover, there are potential biochemical and technical applications based on the formation of adducts between transition metal complexes of Re^I, Ru^{II}, Os^{III}, Rh^{III}, or Co^{III} and biological macromolecules such as DNA.[8] As these complexes show exceptionally rich excited-state behavior and redox chemistry as well as thermal and photochemical stability,[9] they have also been used as biological labeling reagents and noncovalent probes for biomolecules and ions.[10] In this regard, some complexes including biologically relevant ligands, such as substituted pterins, coordinated to the $Re(CO)_3Cl$ core have been synthesized and characterized.[11,12] Pterins (2-amino-4-oxo-3*H*-pteridine, Scheme 1) are heterocyclic compounds widely distributed in nature. Pterin derivatives substituted at the 6-position are usually found in biological systems such as

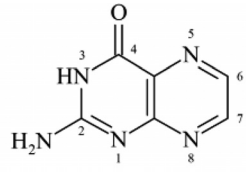

2-amino-4-oxo-3*H*-pteridine (pterin)

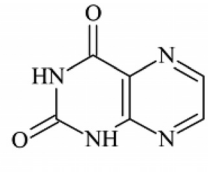

2,4-dioxo-1*H*,3*H*-pteridine (lumazine)

Scheme 1.

[a] Instituto de Investigaciones Fisicoquímicas Teóricas y Aplicadas (INIFTA, UNLP, CCT La Plata-CONICET), Diag. 113 y 64, Sucursal 4, C.C. 16, (B1906ZAA) La Plata, Argentina
E-mail: gruiz@inifta.unlp.edu.ar
ewolcan@inifta.unlp.edu.ar
[b] Departamento de Física, Facultad de Ciencias Exactas, Universidad Nacional de La Plata e IFLP (CONICET, CCT-La Plata), C.C. 67, (1900) La Plata, Argentina
[c] IIB-INTECH-CONICET, Universidad Nacional de San Martín, Intendente Marino km 8.2 C.C. 164, (B7130IWA) Chascomús, Buenos Aires, Argentina
[d] CIHIDECAR-CONICET, Departamento de Química Orgánica, Facultad de Ciencias Exactas y Naturales, Universidad de Buenos Aires, Pabellón II, 3er P., Ciudad Universitaria, (1428) Buenos Aires, Argentina
[e] Clean Energy Research Center, University of Yamanashi, 4-3-11 Takeda, Kofu, Yamanashi, 400-8511, Japan
Supporting information for this article is available on the WWW under http://dx.doi.org/10.1002/ejic.201200681.

pigments, one-carbon transfer cofactors, and redox cofactors. Such biological significance has attracted considerable interest in the study of their properties and reactivity in vitro and also in vivo.[13] The binding of the $Re(CO)_3Cl$ fragment to these heterocycles usually occurs through the O4–N5 chelating site.[11] This has been verified for a large number of metal-pteridine complexes, with Cu^{II},[14,15] Zn^{II},[15] Ru^{II},[13a,16] Co^{II},[17] Ni^{II},[18] Fe^{II},[17b] Mo^{VI},[19] Ir^{III},[12a] and others.[20]

The presence of multiple intermolecular hydrogen bonds in metal-containing pterin complexes is responsible for the low solubility of most of the examples found in the literature.[21] For this reason, crystal structure determinations of metal complexes containing pterin ligands are scarce in the literature.

Most of the reported X-ray structures are obtained from metal complexes that contain pterin derivatives like 2-(dimethylamino)-4-oxo-3*H*-pteridine[17b] or lumazine methylated ligands,[11–12] which are more soluble than pterin in water or organic solvents and, therefore, more suitable for the isolation of single crystals. Recently, however, a new pterin complex with a good solubility in water, namely Ni(ethylenediamine)(pterin)$_2$, has been synthesized and its structure was determined by X-ray diffraction.[21] To the best of our knowledge, there are still no examples of crystal structures of $XRe(CO)_3L$ complexes with pterin ligands. Here, we present the synthesis of a new water-soluble complex, $Re(CO)_3(pterin)(H_2O)$, along with its structural and spectroscopic characterization. In this complex, the Re^{I} ion is in a slightly distorted octahedral environment, coordinated to a planar pterin. Strong H bonds between the hydrogen atom of the 2-amino group and crystallization water molecules gives rise to a polymeric arrangement with neighboring $Re(CO)_3(pterin)(H_2O)$ complexes linked in the solid state. The Re^{I} complex was also characterized by using ^1H NMR and FTIR spectroscopy, and by a combination of three mass spectrometry techniques: matrix-assisted laser desorption/ionization (MALDI), electrospray ionization (ESI), and probe electrospray ionization (PESI). Despite the fact that the use of MS in the field of organometallic chemistry has been significantly extended,[22] the application of PESI-MS for the analysis of organometallic compounds was only achieved very recently.[23] To complete the characterization of the Re^{I}-pterin complex, protonation studies were performed in its aqueous solutions by following the behavior of UV/Vis absorption spectra within the 2–11 pH range. With the aid of chemometric methods, two pK_a values could be obtained from the protonation studies, namely pK_{a1} = 3.9 and pK_{a2} = 8.8.

Results and Discussion

Spectroscopic Characterization

The Re pterin complex was obtained in good yield and it was characterized by elemental analysis, FTIR and ^1H NMR spectroscopy, MALDI and ESI mass spectrometry, and structural X-ray diffraction methods. The IR absorption spectrum is consistent with both the facial configuration of the carbonyl ligands and with its C_s symmetry, as revealed by the presence of two intense absorptions bands in the 2050–1880 cm^{-1} region. According to previous reports on similar compounds, the sharp band at higher frequency (ca. 2029 cm^{-1}) is attributed to the A′$_1$ mode (totally symmetric in-phase stretching of the three CO ligands), whereas the remaining two bands at intermediate and lower frequencies (1901 and a shoulder at 1941 cm^{-1}), are assigned to the A′$_2$ (totally symmetric out-of-phase stretching) and A″ modes (asymmetric stretching of the equatorial CO ligands).[7b,24]

As sometimes observed in *fac*-[$Re(CO)_3(L)(L')$]-type complexes, in the case of $Re(CO)_3(pterin)(H_2O)\cdot 2H_2O$, the A′$_2$ and A″ bands are superimposed into a single broad band,[25] and only a shoulder is observed adjacent to the strong band centered at 1901 cm^{-1}. This pattern is in agreement with the low symmetry expected around the metal center in the complex. Compared to the free pterin ligand (C4=O4 stretches at 1619, 1692, and 1726 cm^{-1}), the complex showed significant shifts to lower frequencies in the region 1600–1800 cm^{-1}. These are typical features that indicate deprotonation of the N3 atom in the pterin ligand and, hence, complexation through O4 and N5.[21]

In the ^1H NMR spectrum, the two doublet signals in the complex corresponding to C6–H and C7–H protons are shifted to lower fields relative to the signals of free pterin, because of the heavy atom effect exerted by the Re atom. This coordination effect upon δ has been previously observed in related pteridine complexes.[11] However, the coordination through O4 and N5 shifts the C2–NH_2 singlet signal to higher field. An additional doublet signal at 7.21 ppm was observed in the Re complex. When drops of D_2O are added to the DMSO solution of the complex, both the C2–NH_2 and the 7.21 ppm signals disappear. In the case of C2–NH_2 signal, the D_2O effect is due to the interchangeable nature of such a proton, whereas in the case of the signal at 7.21 ppm the effect could be assigned to the interchange of coordinated H_2O with D_2O. The absence of the ^1H NMR signal of N3–H in the Re complex is indicative of coordination through O4 and N5.

High flow ESI with the assistance of corona discharge (HF-ESI-CD) taking place at the tip of the electrospray capillary was used to avoid decomposition of the rhenium complexes and to induce specifically one electron exchange (oxidation or reduction). Figure 1a shows the HF-ESI-CD mass spectrum in positive ion mode of the complex under study. The intact molecular ion $[M]^+$ at m/z = 451.04 was observed, as well as the fragment formed when a water ligand is lost $[M - H_2O + H]^+$ at m/z = 434.07. In the spectrum, contributions from ^{187}Re and ^{185}Re (62.6 and 37.4% natural abundance, respectively) to the intact molecular ion and to the fragment formed when a water ligand is lost can be clearly observed at m/z = 451.04, 449.03 and 434.07, 432.08 for $[M]^+$ and $[M - H_2O + H]^+$, respectively. Figure 1b shows the MS/MS spectrum obtained when pulsed Q collision induced dissociation (PQD) mode was used. The

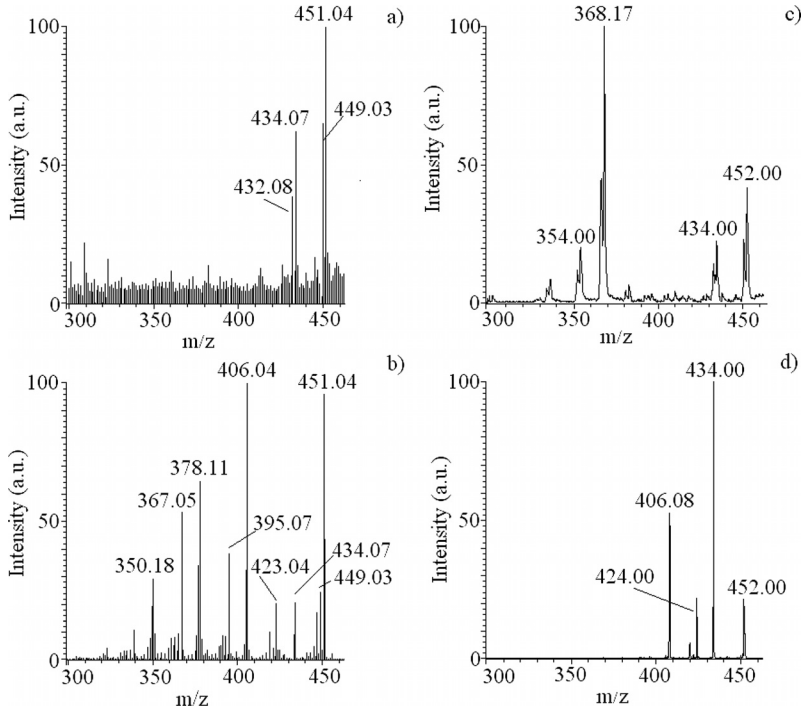

Figure 1. Positive ion mass spectra of $Re(CO)_3(pterin)(H_2O)$: a) HF-ESI-CD b) HF-ESI-CD-MS/MS c) PESI d) PESI-MS/MS.

signals observed correspond to $[M - H_2O + H]^+$ at m/z = 434.07, $[M - CO]^+$ at m/z = 423.04, $[M - H_2O - CO + H]^+$ at m/z = 406.04, $[M - 2(CO)]^+$ at m/z = 395.07, $[M - H_2O - 2(CO) + H]^+$ at m/z = 378.11, $[M - 3(CO)]^+$ at m/z = 367.05, and $[M - H_2O\ 3(CO) + H]^+$ at m/z = 350.18. By using HF-ESI-CD, it is possible to fully characterize the complex under study. In negative ion mode, even when HF-ESI-CD was used, the intact molecular ion was not detected (result not shown). The principal signal observed corresponds to $[M - H_2O - H]^-$ at m/z = 432.15, which can be used as a structural diagnosis signal/fragment.

Probe electrospray ionization (PESI) is a recently developed ionization technique, in which a solid needle is used as the sampling probe and electrospray ionization emitter instead of a capillary.[26] A solid stainless needle or wire is adopted to repeatedly load a small amount of sample solution by dipping the needle tip into the solutions. Then, an electrospray will be generated when a high voltage (i.e., 3 kV) is applied to the needle. PESI-MS was successfully applied for characterization of a number of rhenium complexes.[23] Figure 1c shows the PESI mass spectrum of $Re(pterin)(CO)_3(H_2O)$. The intact molecular ion $[M + H]^+$ at m/z = 452.00, the fragment formed when a water ligand is lost $[M - H_2O + H]^+$ at m/z = 434.00, and the one formed when CO ligands are lost $[M - 3(CO) + H]^+$ at m/z = 368.17 were observed. Two others fragments were observed when MS/MS analysis was performed, $[M - CO + H]^+$ at m/z = 424.00 and $[M - H_2O - CO + H]^+$ at m/z = 406.08 (Figure 1d). Both ionization methods used allowed the detection of the intact molecular ion, however a higher signal-to-noise ratio was observed when PESI was used instead of HF-ESI-CD-MS.

As $Re(CO)_3(pterin)(H_2O)$ shows strong absorption in the UV/Vis region (see below), particularly at 355 nm, laser desorption/ionization (LDI) MS, without the presence of a secondary molecule as photo-sensitizer or matrix in the sample, was used. As shown in Figure S1a and d, the intact molecular ion of this complex could not be detected in positive or negative ion mode. However, information about the structure of the complex was obtained from structural diagnosis signals. In positive ion mode $[M - H_2O - 2(CO) + H]^+$ at m/z = 378.20, $[M - 3(CO) + H]^+$ at m/z = 368.05, and $[M - H_2O - 3(CO) + H]^+$ at m/z = 350.25 were detected, whereas in negative ion mode $[M - H_2O - H]^-$ at m/z = 432.27 was observed.

A MALDI mass spectra of $Re(CO)_3(pterin)(H_2O)$ was recorded using norharmane (nHo) and 2-[(2E)-3-(4-*tert*-buthylphenyl)-2-methylprop-2-enylidene] malononitrile (DCTB) as matrices. Both matrices have been previously used for analysis of rhenium complexes[23,27] and allowed the detection of, in some cases with very low intensity, intact molecular ions of those complexes. However, for this particular complex, the intact molecular ion could not be detected with either of these matrixes in negative or positive ion mode. As shown in Figure S1b and c, for positive ion mode, at least some characteristic fragments were observed. In addition to the fragments detected by LDI-MS, $[M - H_2O + H]^+$ at m/z = 434.07 was observed. MALDI-MS for the complex in negative ion mode is shown in Figure S1e and f. The most intense signal corresponds to $[M - H_2O - H]^-$ at m/z = 432.27. Although MALDI-MS is a softer ionization technique than LDI-MS, it was not possible to detect the intact molecular ion of the complex under study, and only fragments produced for the loss of

one or more ligands were detected. The obvious reason was that this analyte absorbs part of the laser photons, and as consequence, it is almost impossible to find a proper matrix.

Structural Characterization

Figure 2 shows ORTEP[28] plots of the $Re(CO)_3$(pterin)$(H_2O)\cdot 2H_2O$ complex. The crystal data and structure refinement results are summarized in Table 1. The intramolecular bond lengths and angles around the metal are given in Table 2. [Note the discrepancy between the numbering according to heterocyclic nomenclature (Scheme 1) and the numbering in Figure 2 and Table 2 from the present crystal structure analysis].

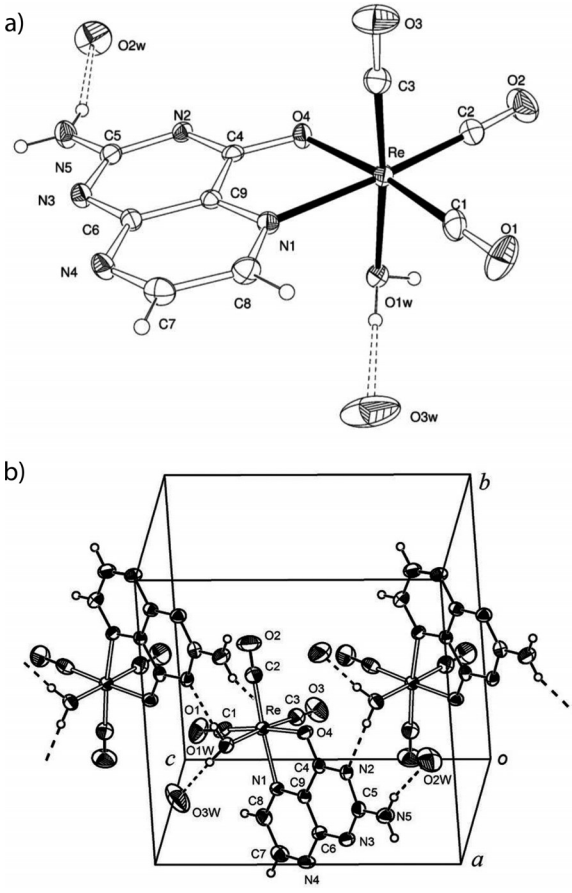

Figure 2. a) View of $Re(CO)_3$(pterin)$(H_2O)\cdot 2H_2O$ molecule showing the labeling of the non-H atoms and their displacement ellipsoids at the 50% probability level. Metal–ligand bonds are indicated by filled lines and H bonds by dashed lines. b) Projection of $Re(CO)_3$(pterin)$(H_2O)\cdot 2H_2O$ showing the crystal packing. The figure displays the H bonds that link neighboring $Re(CO)_3$(pterin)$(H_2O)\cdot 2H_2O$ complexes in a polymer extending along the *c* axis.

The Re^I ion is in a slightly distorted octahedral environment. A planar pterin anion coordinated to the metal defines an equatorial plane (rms deviation of atoms from the least-squares plane of 0.012 Å) and acts a bidentate ligand through its carbonyl oxygen and N atoms [*d*(Re–O) 2.162(3) Å, *d*(Re–N) 2.186(3) Å, ∠(O–Re–N) 76.6(1)°]. Two CO groups lie at *cis* positions nearly onto this plane [Re–C distances 1.896(6) and 1.920(5) Å]. The apical positions of the octahedron are occupied by a third CO group [*d*(Re–C) 1.889(5) Å] and a water molecule [*d*(Re–Ow) 2.190(3) Å]. The Re–(CO) bonds are nearly perpendicular to each other [OC–Re–CO angles in the 88.9(2)–89.1(2)° range].

Table 1. Crystal data and structure refinement results for $Re(CO)_3$(pterin)$(H_2O)\cdot 2H_2O$.

Empirical formula	$C_9H_{10}N_5O_7Re$
Formula weight	486.42
Temperature	295(2)
Wavelength	0.71073
Crystal system	monoclinic
Space group	$P2_1/c$
Unit cell dimensions	a = 11.9165(5) Å
	b = 10.5694(4) Å
	c = 11.0357(4) Å
	β = 96.423(4)°
Volume	1381.22(9) Å^3
Z, density (calculated)	4, 2.339 mg/m^3
Absorption coefficient	8.843 mm^{-1}
F(000)	920
Crystal size	0.34 × 0.21 × 0.11 mm
θ range for data collection	3.07 to 25.99°.
Index ranges	$-14 \le h \le 8$, $-13 \le k \le 6$, $-11 \le l \le 13$
Reflections collected	5045
Independent reflections	2709 [R(int) = 0.0202]
Observed reflections	2188
Completeness to θ = 25.99°	99.8%
Max. and min. transmission	0.4485 and 0.1540
Refinement method	full-matrix least-squares on F^2
Data/restraints/parameters	2709/3/207
Goodness-of-fit on F^2	0.953
Final R indices [$I > 2\sigma(I)$]	R_1 = 0.0223, $wR2$ = 0.0502
R indices (all data),[a],[b]	R_1 = 0.0303, $wR2$ = 0.0514
Largest diff. peak and hole	0.817 and –0.866 e Å^{-3}

[a] $R_1 = \Sigma||F_o| - |F_c||/\Sigma|F_o|$. [b] $wR_2 = [\Sigma w(|F_o|^2 - |F_c|^2)^2/\Sigma w(|F_o|^2)^2]^{1/2}$.

Table 2. Bond lengths [Å] and angles [°] around the Re ion in $Re(CO)_3$(pterin)$(H_2O)\cdot 2H_2O$.[a]

Bond length	[Å]	Angle	[°]
Re–C(3)	1.889(5)	C(3)–Re–C(1)	89.1(2)
Re–C(1)	1.896(6)	C(3)–Re–C(2)	88.8(2)
Re–C(2)	1.920(5)	C(1)–Re–C(2)	89.1(2)
Re–O(4)	2.162(3)	C(3)–Re–O(4)	95.04(17)
Re–N(1)	2.185(3)	C(1)–Re–O(4)	173.66(17)
Re–O(1W)	2.190(3)	C(2)–Re–O(4)	95.85(17)
		C(3)–Re–N(1)	92.90(17)
		C(1)–Re–N(1)	98.37(17)
		C(2)–Re–N(1)	172.39(17)
		O(4)–Re–N(1)	76.62(12)
		C(3)–Re–O(1W)	174.55(16)
		C(1)–Re–O(1W)	94.71(18)
		C(2)–Re–O(1W)	95.15(17)
		O(4)–Re–O(1W)	80.88(12)
		N(1)–Re–O(1W)	82.67(12)

[a] Note that the crystallographic numbering (Figure 2) differs from the numbering according to the heterocyclic nomenclature (Scheme 1).

Upon coordination to a Re^{I} ion, the neutral pterin (2-amino-4-oxo-3*H*-pteridine) molecule loses the proton at the 3-position to become an anionic pterin ligand. As a consequence, the –(N2H)–C4=O4 bonding structure changes from formally a single and a double bond to –N2=C4=O partial double bonds with a shortening of the N2–C4 bond from the usual N–C distances (in the 1.35–1.37 Å range) to a value of 1.326(6) Å and a corresponding lengthening of the C4=O4 bond (in the range from 1.20 to 1.24 Å) to a value of 1.283(5) Å; this later effect is enhanced by the Re–O4 interaction.

The conformation of $Re(CO)_3(pterin)(H_2O)$ resembles the one found in the related $Re(6\text{-ATML})(CO)_3Cl$ complex,[11] in which the pterin ion is replaced by the uncharged 6-ATML (6-acetyl-1,3,7-trimethyllumazine) ligand and the coordination water by a chloride ion. As expected, the Re–O and Re–N bond lengths in our complex are slightly shorter [by 0.027(4) and 0.037(4) Å, respectively] than the corresponding bond lengths of the latter one.

Neighboring $Re(CO)_3(pterin)(H_2O)$ complexes related through a crystallographic glide plane are linked to each other by a strong Ow–H···N bond [*d*(Ow···N2′) 2.826 Å, ∠(Ow-H···N2′) 166.7°], which gives rise to a polymeric arrangement that extends along the crystallographic *c* axis (Figure 2b). Another H bond occurs between one amine hydrogen atom of N5 and the oxygen atom of a crystallization water molecule. This intermolecular H bond makes the amino nitrogen atom more negatively charged due to the polarization of the N–H bond of the amino group, resulting in the stabilization of a resonance structure (R2 over R1 in Scheme 2) with a quinonoid form, which gives a double bond character to C5–N5. This stabilization of a resonance structure with a quinonoid character has been previously observed with a Ru^{II}-pterin complex.[16b] Moreover, the C5–N5 distance (1.327 Å) is very similar to the C4–N2 distance (1.326 Å), which has a partial double bond character. In fact, the C4–N2 distance is close to the shortest C–N distances found in the pterin ring. Further details of the H-bonding structure are provided as Supporting Information (Table S1).

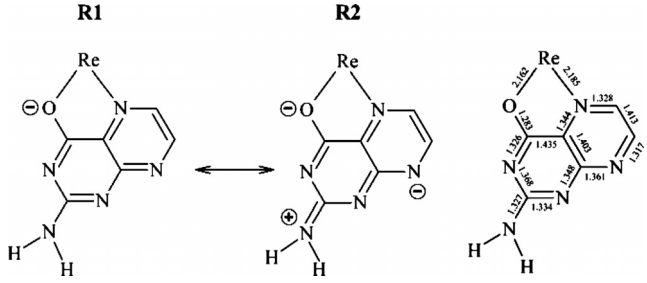

Scheme 2.

UV/Vis Absorption Spectroscopy

Theoretical calculations have shown that the highest occupied molecular orbital (HOMO) in *fac*-$XRe(CO)_3L$ complexes corresponds to an orbital mainly localized at the Re center with some delocalization over X ligands. This delocalization also accounts for the mixing of intraligand (IL) and metal-to-ligand charge-transfer (MLCT) states. On the other hand, the lowest unoccupied molecular orbital (LUMO) is localized exclusively on the L ligand.[24]

The absorption spectrum of $Re(CO)_3(pterin)(H_2O)$ in alkaline media, i.e. at pH 11, consists of one intense ($\varepsilon \approx 2 \times 10^4$ $M^{-1}cm^{-1}$) absorption centered at λ_{max} = 255 nm and an absorption band of medium intensity ($\varepsilon \approx 6 \times 10^3$ $M^{-1}cm^{-1}$) centered at 373 nm. In neutral solutions (pH 7), the high energy band remains virtually unaffected, whereas the low energy band shifts to λ_{max} = 366 nm. In acidic media (pH 2) the band at λ_{max} = 255 nm has disappeared and only a tail remains in the 220–300 nm region, whereas in the 300–500 nm region, two bands can be observed: the first one, λ_{max} = 344 nm, and the second one appearing as a broad shoulder, centered at λ_{max} ca. 360–370 nm. The invariance of the UV/Vis spectra upon going from pH 2 to 11 and then reversing to pH 2 suggests that no dissociation of ligands occurs after pH changes and that the complex is stable in the whole pH range studied. Therefore, a reversible protonation–deprotonation behavior is witnessed in the UV/Vis spectrum of the Re^{I} complex as the pH is changed between 2 and 11. In addition, aqueous solutions showed no spectral changes upon storage for 48 h, which shows the stability of the complex within this timescale.

Figure 3a shows the spectral changes observed between pH 2 and 7; isosbestic points can be observed at 243, 287, 355, and 422 nm. On the other hand, isosbestic points are observed at 270, 285, and 307 nm in the pH range between 7 and 11 (Figure 3b). Figure 3c shows the absorption spectra of the acid/base forms of pterin at pH 2, 6, and 11. The spectrum of the Re^{I} complex can be compared to the one of free pterin. At pH 2 and 11, both spectra have similar shape and band maxima, even though the bands of the Re^{I} complex are broader than the ones of free pterin. This broadening in the absorption bands of the Re^{I} complex is quite noticeable in the visible region of the spectrum: the absorption spectrum of pterin extends up to 425 nm, whereas the one of the Re^{I} complex reaches 525 nm. The spectral features of free pterin in its acidic form at pH 6 (λ_{max} = 270 nm and a low energy band centered at λ_{max} = 340 nm) are absent in the absorption spectra of the Re^{I} complex acidic solutions. In the Re^{I} complex, these spectral features are in agreement with those found in the electronic spectrum of the pterinate/pterin species[13b] (assigned to π–π* excitations in the aromatic ligand fragment) plus electronic transitions of MLCT character (which may be responsible for the broadening of the spectral features mentioned above).

The analysis of the full (augmented) matrix of the UV/Vis spectra in Figure 3a and b was performed by using chemometric techniques. Both factor analysis and singular value decomposition were used for the estimation of the number of independent contributions yielding *n* values of 3. An orthogonal projection approach was used to obtain initial guesses of the spectra corresponding to each contrib-

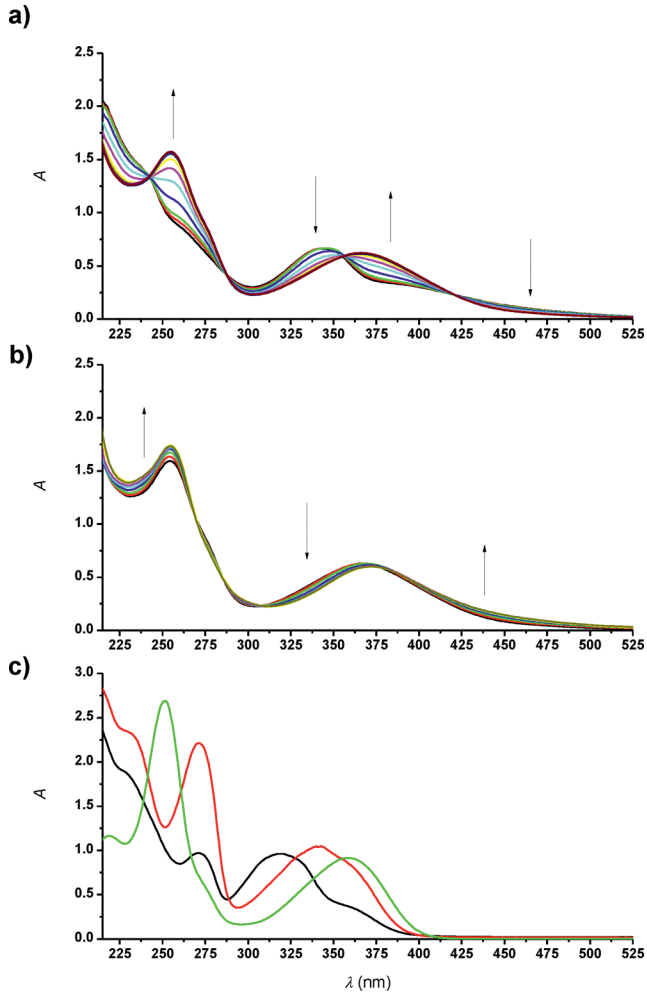

Figure 3. UV/Vis spectral changes displayed by $Re(CO)_3$(pterin)(H_2O) in protonation studies. a) Spectral changes in the 2–7 pH range: black pH 2, red pH 2.5, green pH 3, blue pH 3.5, cyan pH 4, magenta pH 4.5, yellow pH 5, dark yellow pH 5.5, navy pH 6, purple pH 6.5, wine pH 7. b) Spectral changes in the 7.5–11 pH range: black pH 7.5, red pH 8, green pH 8.5, blue pH 9, cyan pH 9.5, magenta pH 10, yellow pH 10.5, dark yellow pH 11. c) UV/Vis spectra of pterin at pH 2 (black), 6 (red), and 11 (green). See text for details.

uting species.[29] The spectral shapes obtained by using a multivariate curve resolution-alternating least squares (MCR-ALS) method for the three species are shown in Figure 4. The inset of Figure 4 shows the distribution functions for the three species over the whole pH range. From this figure two pK_a values, 3.9 and 8.8, can be obtained. In aqueous solutions, pterin behaves as a weak acid and the amide group is in equilibrium with the phenolate group, Scheme 3, with a pK_a of ca. 8.[13b] In a related Ru^{II} complex containing a pterin derivative, the protonation of the complex has been ascribed to the protonation of the N3 group in the coordinated pterin ring.[16a] The acidity of the N3–H proton in the complex is considerably higher, relative to the acidity of the N3–H proton in free pterin, by about four pK_a units.[16a] This comparatively strong response of the pKa(NH) on coordination to a positively charged metal complex fragment has been explained in terms of the vicinity of the acidic NH group in the α position to the metal coordinating carbonyl group.[16a] Therefore, in our pterin complex, the pK_{a1} = 3.9 can be assigned to the protonation equilibrium of N3, which suggests that there is a considerable electronic coupling between the Re chelate ring and the N3 site.[16a] A tautomerization equilibrium between amidate and imidate forms has been suggested.[16b] However, in Scheme 4, for the sake of simplicity, only the imidate form has been considered for the protonation of the N3 site.

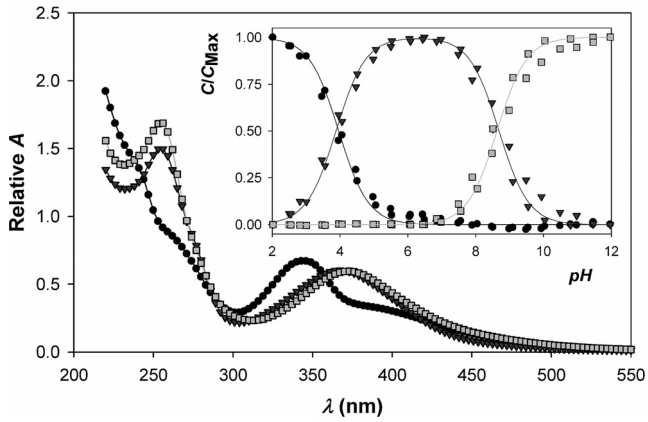

Figure 4. Spectral shapes for the three species and their distribution functions obtained from chemometric analysis of UV/Vis spectral changes displayeded by $Re(CO)_3$(pterin)(H_2O) in protonation studies (Figure 3a and b). Circles species 1, down triangle species 2, square species 3. See text for details.

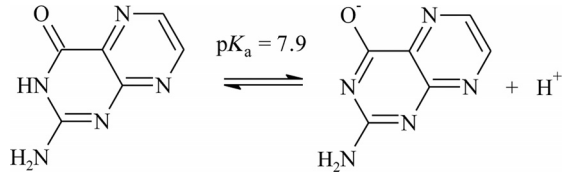

Scheme 3.

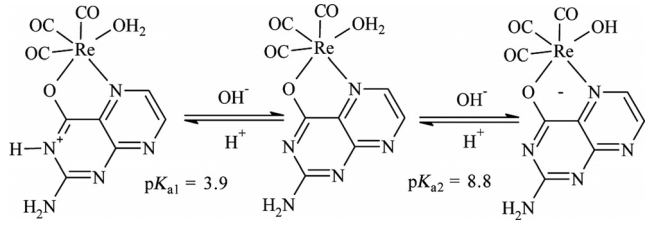

Scheme 4.

As the spectral changes observed between pH 7 and 11 are much smaller than those observed between pH 2 and 7, and given that free pterin has no acid/base forms in equilibrium above pH 8, the second equilibrium observed with the Re^{I} complex, pK_{a2} = 8.8, could be ascribed to deprotonation of a coordinated water molecule to yield the hydroxo complex, Scheme 4. In fact, the species that predominates at pH 11 has spectral features only compatible with the basic form of pterin.[13b]

Solutions of the $Re(CO)_3(pterin)(H_2O)$ complex in aprotic solvents like acetonitrile and/or methanol displayed small spectral changes in the 300–500 nm range, which were ascribed to the replacement of the water molecule by an organic solvent molecule in the Re^I complex. Those small spectral changes occurred within two hours after the dissolution of Re^I complex. After that time period, the UV/Vis spectrum remained stable. Similar successive water molecule replacements were observed when aqueous solutions of $[Re(CO)_3(H_2O)_3]^+$ were mixed with monodentate ligands such as dimethyl sulfoxide and acetonitrile.[30] Further studies are underway in order to evaluate the aprotic solvent effects on the photophysical properties of $Re(CO)_3(pterin)(H_2O)$.

Conclusions

A new Re^I coordination compound that includes the unsubstituted pterin ligand, $Re(CO)_3(pterin)(H_2O)$, has been obtained successfully. Evidence for the coordination of the pterin ligand through the O4 and N5 atoms was obtained by ^1H NMR and FTIR spectroscopy. Structural characterization by X-ray diffraction confirmed the binding mode of pterin and also showed the three carbonyl ligands in a facial conformation. The octahedral coordination of the central metal atom is completed by a water molecule. Two additional water molecules of crystallization are involved in a hydrogen-bonding network that extends along the crystal and links neighboring complexes. As far as we know, this polymeric arrangement has not been reported before for any tricarbonylrhenium complexes with pterin ligands. The structural analysis was deepened by the comparative use of a combination of three mass spectrometry techniques. In general, more efficient fragmentation or decomposition of the analytes was observed when laser desorption/ionization methods (LDI and MALDI) were used. ESI methods, the most used MS technique in the field of organometallic chemistry, showed the intact molecular ion and additional structural information that can be utilized as structural diagnosis signals/fragments. Moreover, we demonstrated in this work for the first time that PESI, a recently developed ionization technique, is also useful for the study of Re-pterin complexes. Both ESI methods used allowed us to detect the intact molecular ion, however a higher signal-to-noise ratio was observed when PESI was used instead of ESI.

Interesting features concerning this particular $Re(CO)_3(pterin)(H_2O)$ complex are both its relatively high solubility in water and its remarkable stability in the entire pH range studied. The former may be an important property in relation to its applications in radiopharmacy.[31] The absorption bands could be assigned to contributions from individual states of the ligand, IL transitions, and metal-to-ligand charge-transfer transitions. The presence of protonation–deprotonation processes in $Re(CO)_3$ complexes is unusual. We have reported in this work two acid–base equilibriums in a Re-pteridine complex. pK_{a1} = 3.9 was assigned to the protonation equilibrium of the pterin ligand in the complex and pK_{a2} = 8.8 could be ascribed to deprotonation of a coordinated water molecule.

Experimental Section

General: HPLC-grade methanol (Kanto Chemical CO INC, Japan), ethanol, and acetonitrile (J. T. Baker, USA) were used without further purification. 9*H*-Pyrido[3,4-*b*]indole (norharmane; nHo), β-cyclodextrin (cyclomaltoheptaose), $ClRe(CO)_5$, and 2-amino-4-oxo-3*H*-pteridine (pterin) were purchased from Sigma–Aldrich Chemical Co., USA. 2-[(2*E*)-3-(4-*tert*-Butylphenyl)-2-methylprop-2-enylidene]malononitrile (DCTB) was purchased from Fluka Sigma–Aldrich, Switzerland. Water of very low conductivity (Milli Q grade) was used.

Synthesis: The Re^I–pterin complex was prepared by a modification of procedures reported for the synthesis of similar Re complexes.[11–12,20] A 100 mL round-bottomed flask was loaded with a solution of pterin (181 mg, 1.1×10^{-3} mol) in water (75 mL), and the resulting colorless solution was heated at ca. 60 °C. Then, an ethanolic solution (75 mL) of $ClRe(CO)_5$ (362 mg, 1.0×10^{-3} mol) was slowly added to the vigorously stirred hot aqueous solution. The mixture was heated to reflux for 7 h under a N_2 atmosphere, and the initially colorless liquid turned orange. The slight excess of pterin, an insoluble white powder, was removed by filtration. The solution was then cooled to room temperature, and the solvents evaporated to dryness. The resulting solid was dissolved in a minimum volume of dichloromethane, and the complex was precipitated by the slow addition of cold iso-octane. The recrystallization procedure was repeated until a constant value was obtained for the molar absorption coefficient. The obtained orange solid was dried under vacuum. Pterin complexes are known to cocrystallize with solvent molecules.[11] In our case, after the crystallization from CH_2Cl_2 a cocrystallization of 2.5 solvent molecules was evident from the elemental analysis results; yield 334 mg (70%). $Re(CO)_3(pterin)(H_2O)\cdot 2.5CH_2Cl_2$: calcd. H 1.3, C 20.8, N 10.5; found H 1.4, C 20.4, N 10.8. IR (KBr): $\tilde{\nu}$ = 1602 (m), 1623 (m), 1653 (m), 1900 (s), 1940 (s, shoulder), 2029 (s), 3500 (–OH) cm^{-1}. The relevant wavenumbers for pterin are 1619 (m), 1692 (m), and 1726 (m) cm^{-1}. ^1H NMR, Re complex (500 MHz, [D$_6$]DMSO): δ = 8.93 (*d*, *J* = 2.5 Hz, 7-H), 8.79 (d, *J* = 2.5 Hz, 6-H), 7.56 (s, C2–NH_2) ppm. ^1H NMR, pterin (500 MHz, [D$_6$]DMSO): δ = 8.79 (d, *J* = 2.5 Hz, 7-H), 8.70 (d, *J* = 2.5 Hz, 6-H), 8.52 (s, C4-OH), 8.35 (s, C2-NH_2) ppm. The N3–H ^1H NMR signal was not observed neither in the spectra corresponding to the free pterin moiety nor in the Re complex.

Instrumentation: UV/Vis spectra were recorded with a Shimadzu UV-1800 spectrophotometer. FTIR spectra were recorded with a Nicolet 8700 Thermo Scientific instrument. pH measurements were performed with a Adwa AD8000 pH meter. ^1H NMR spectra of pterin and Re complex solutions were recorded at 300 K with a Bruker AM-500 spectrometer operating at 500 MHz. [D$_6$]DMSO was used as a solvent and the chemical shifts were referenced relative to the $(CH_3)_2SO$ in [D$_6$]DMSO (δ =2.50 ppm). Typically, solutions were introduced into a 5 mm diameter tube.

Ionization Techniques

PESI-MS Analysis: The probe electrospray ionization (PESI) experimental procedures were described previously.[26,32] Briefly, the needle was moved up and down along a vertical axis using a custom-made linear actuator system. When the needle was at the bottom position, the tip of the needle was adjusted to touch the sur-

face of the liquid sample. When the needle was moved up to the highest position, a high voltage of about 2–3 kV was applied to it. The distance of the needle stroke was 10 mm. As electrospray emitters, disposable acupuncture needles (Seirin, Shizuoka, Japan) with submicrometer tip diameter were used throughout the PESI-MS experiments. The PESI mass spectra were obtained with an acquisition time of 1 s with a probe motion frequency of 3 Hz.

The ions generated from the electrospray were sampled through the ion-sampling orifice with a diameter of 0.4 mm into the vacuum chamber and mass-analyzed by a linear ion trap mass spectrometer (LTQ-Velos, Thermo Scientific, USA) equipped with collision-induced dissociation (CID) and pulsed Q collision induced dissociation (PQD) modes.

Stock solutions of the complex were prepared in methanol at a concentration of 10^{-4} M. Dilutions were prepared from stock solutions. Each experiment was repeated at least three times in order to ensure reproducibility. Spectra were obtained and analyzed with the program Thermo Xcalibur Qual Browser.

ESI-MS Analysis: ESI-MS analyses were performed with a linear ion trap mass spectrometer (LTQ-Velos, Thermo Scientific, USA) equipped with CID and PQD modes and operated in the negative or positive ion mode. High flow electrospray with the assistance of corona discharge taking place at the tip of the electrospray capillary was used to avoid decomposition (interchange of ligands and solvent) of the rhenium complex and to induce ionization of neutral analytes.[23,33] The source voltage applied was 8 kV, the source current 15 μA, the sheath gas flow rate was 30 (arbitrary units), and the capillary temperature was 150 °C. Ion optics parameters: multipole 00 offset: –3.3 V, lens 0: –6.2 V, multipole 0 offset: ±6.3 V, lens 1: –9.2 V, gate lens: –91.9 V, multipole 1 offset: –6.6 V, and multi-pole RF amplitude: 602.3 (Vp-p). A syringe pump (Agilent, USA) with 2.3 mm diameter was used to introduce the sample at a flow rate of 10 μL/min. Stock solutions of the complex were prepared in methanol at a concentration of 10^{-4} M. Diluted solutions were prepared from the stock solutions. Each experiment was repeated at least three times in order to ensure reproducibility. Spectra were obtained and analyzed with the program Thermo Xcalibur Qual Browser.

MALDI-TOF/TOF MS and LDI-TOF/TOF MS Analysis: The Re complex was analyzed by ultraviolet matrix assisted laser desorption-ionization mass spectrometry (UV–MALDI MS) and by ultraviolet laser desorption-ionization mass spectrometry (UV–LDI MS) performed with a Bruker Daltonics Ultraflex II TOF/TOF mass spectrometer (Leipzig, Germany). Mass spectra were acquired in linear positive and negative ion modes and with the LIFT device in the MS/MS mode. Stock solutions of complex (10^{-4} M) were prepared in water. These solutions were then diluted 10- to 100-fold to final concentrations from 10^{-5} to 10^{-6} M. External mass calibration was made by using β-cyclodextrin (MW 1134) with norharmane (nHo) as the matrix in positive and negative ion mode. The matrix signal was used as an additional standard for calibration in both ionization modes. Sample solutions were spotted on a MTP 384 polished stainless steel target plate from Bruker Daltonics (Leipzig,Germany). For UV–MALDI MS, matrix solutions were prepared by dissolving nHo (1 mg/mL) in acetonitrile/water (1:1, v/v) solution, and DCTB[27] (10 mg/mL) in dichloromethane. For UV-MALDI MS experiments, dry droplet sample preparation or the sandwich method was used according to Nonami et al.,[34] i.e., loading successively 0.5 μL of matrix solution, analyte solution, and matrix solution after drying each layer in a normal atmosphere and at room temperature. The matrix to analyte ratio was 3:1 (v/v), and the matrix and analyte solution loading sequence was: i) matrix, ii) analyte, iii) matrix, iv) matrix. For UV-LDI MS experiments two portions of analyte solution (0.5 μL × 2) were loaded on the probe and dried successively (two dry layers). Desorption/ionization was obtained by using the frequency-tripled Nd:YAG laser (355 nm). The accelerating potential was 20 kV. Experiments were performed using, firstly, the full-range setting for the laser firing position in order to select the optimal position for data collection, and secondly fixing the laser firing position in the sample sweet spots. The laser power was adjusted to obtain high signal-to-noise ratio (S/N) with minimal fragmentation of the parent ions; each mass spectrum was generated by averaging 100 lasers pulses per spot. Spectra were obtained and analyzed with the programs FlexControl and FlexAnalysis, respectively.

X-ray Diffraction Data: Single crystals of $Re(CO)_3(pterin)(H_2O)\cdot 2H_2O$ were obtained by slow evaporation of a concentrated dichloromethane solution of the Re complex capped with a layer of water. The measurements were performed with an Oxford Xcalibur, Eos, Gemini CCD diffractometer with graphite-monochromated Mo-K_α (λ = 0.71073 Å) radiation. X-ray diffraction intensities were collected (ω scans with θ and κ offsets), integrated, and scaled with CrysAlisPro[35] suite of programs. The unit cell parameters were obtained by least-squares refinement (based on the angular settings for all collected reflections with intensities larger than seven times the standard deviation of measurement errors) using CrysAlisPro. Data were corrected empirically for absorption employing the multi-scan method implemented in CrysAlisPro. The structure was solved by direct methods with SHELXS-97[36] and the molecular model refined by full-matrix least-squares procedure on F^2 with SHELXL-97.[37] The H atoms of the organic ligand were positioned stereochemically and refined with the riding model. The hydrogen atoms of the metal-coordinated water molecule were located in a difference Fourier map and refined isotropically at their found positions with Ow–H and H···H distances restrained to target values of 0.86(1) and 1.36(1) Å, respectively. The crystallization water molecules showed positional disorder. Therefore, their H atoms could not be determined reliably and they were not included in the final molecular model. CCDC-813774 contains the supplementary crystallographic data for this paper. These data can be obtained free of charge from The Cambridge Crystallographic Data Centre via www.ccdc.cam.ac.uk/data_request/cif.

Protonation Studies and Spectroscopic Analysis: pK_a values were determined by spectrophotometric pH titrations using Britton and Robinson's buffer (a mixture of acetic, perchloric, phosphoric and boric acids, each 0.04 M). In each experiment, a solution (25 mL) containing the Re^I complex ([Re] = 9.4×10^{-5} M or 2.7×10^{-5} M), initially at pH 1.9, was increased to pH 12 by addition of 3 M NaOH. After that, the pH was gradually lowered by addition of 50 or 100 μL aliquots of 3 M $HClO_4$, and then the absorption spectrum of each solution was recorded. The procedure was repeated reversing the pH from 1.9 to 12 by adding 50 to 100 μL aliquots of 3 M NaOH. When it was necessary, the absorbances were corrected by the appropriate dilution factors. The pK_a values reported in this work are average values from protonation studies using solutions of the Re^I complex at the two concentrations mentioned above. We used chemometric techniques[38] in order to retrieve, from the absorbance matrix, the concentration profiles and the spectra of each contributing species.[39,40] These methods can be applied to bilinear spectroscopic data from a chemical reaction to provide information about composition changes in an evolving system. In the present work we used the alternating least-squares (ALS) algorithm to simultaneously estimate concentration and spectral profiles.[41] ALS extracts useful information from the experimental data matrix $\mathbf{A}(i\times j)$ by the iterative application of the

following matrix product: $\mathbf{A} = \mathbf{CS}^T + \mathbf{E}$ where $\mathbf{C}(i\times n)$ is the matrix of the concentrations profiles; $\mathbf{S}^T(n\times j)$ is that containing the spectral profiles, and $\mathbf{E}(i\times j)$ represents the error matrix. The indexes i, n, and j denote the sampling pHs, absorbing species, and recorded wavelengths, respectively. Resolving matrix **A** may be a rather difficult task[42] since on the one hand, n is usually unknown[43] and on the other hand, curve resolution methods cannot deliver a single solution because of rotational and scale ambiguities.[44] We applied Factor Analysis and Singular Value Decomposition to the experimental matrix for the estimation of n. In order to reduce rotational ambiguities, we used some chemically relevant constraints[45] such as non-negativity, closure, selectivity, and unimodality. In addition, matrix augmentation strategy was used to simultaneously obtain the concentration profiles corresponding to different experimental conditions.[46]

Supporting Information (see footnote on the first page of this article): Figure S1 and H bond lengths and angles (Table S1).

Acknowledgments

This work was supported in part by Agencia Nacional de Promoción Científica y Tecnológica (ANPCyT) (grant numbers PICT 1482, PME06 2804, and PICT06 2315), Consejo Nacional de Investigaciones Científicas y Técnicas (CONICET) (grant numbers PIP 0389, PIP 1529, and PIP 0400), Universidad de Buenos Aires (X088), and Universidad Nacional de La Plata (UNLP X533) of Argentina. G. P. and R. E. B. would like to thank Mridul K. Mandal and Lee C. Chen at the University of Yamanashi, Japan for their kind help in ESI and PESI-MS experiments. F. R. and G. T. R. thank Dr. Croce and Dr. Peruzzo from INIFTA, UNLP of Argentina for their assistance in FTIR measurements. G. P. thanks CONICET the scholarship for research abroad (Clean Energy Research Center, University of Yamanashi, Kofu, Japan). The Ultraflex II (Bruker) TOF/TOF mass spectrometer was supported by a grant from ANPCyT (PME 125).

[1] M. A. Fox, M. Chanon, *Photoinduced Electron Transfer*, Elsevier, Amsterdam, **1988**.
[2] a) V. Balzani, F. Bolletta, M. Gandolfi, M. Maestri, in: *Organic Chemistry and Theory*, vol. 75, Springer, Berlin/Heidelberg, **1978**, pp. 1–64; b) M. Grätzel, *Energy Resources Through Photochemistry and Catalysis*, Academic Press, New York, **1983**; c) K. Kalyanasundaram, *Coord. Chem. Rev.* **1982**, *46*, 159–244.
[3] K. Kalyanasundaram, M. Grätzel, *Photosensitization and Photocatalysis Using Inorganic and Organometallic Compounds*, Kluwer Academic Publishers, Dordrecht, The Netherlands, **1993**.
[4] a) L. Sacksteder, M. Lee, J. N. Demas, B. A. DeGraff, *J. Am. Chem. Soc.* **1993**, *115*, 8230–8238; b) V. W.-W. Yam, K. M.-C. Wong, V. W.-M. Lee, K. K.-W. Lo, K.-K. Cheung, *Organometallics* **1995**, *14*, 4034–4036; c) D. I. Yoon, C. A. Berg-Brennan, H. Lu, J. T. Hupp, *Inorg. Chem.* **1992**, *31*, 3192–3194.
[5] a) J. C. Calabrese, W. Tam, *Chem. Phys. Lett.* **1987**, *133*, 244–245; b) T. T. Ehler, N. Malmberg, K. Carron, B. P. Sullivan, L. J. Noe, *J. Phys. Chem. B* **1997**, *101*, 3174–3180.
[6] V. W.-W. Yam, V. C.-Y. Lau, K.-K. Cheung, *J. Chem. Soc., Chem. Commun.* **1995**, 259–261.
[7] a) B. Higgins, B. A. DeGraff, J. N. Demas, *Inorg. Chem.* **2005**, *44*, 6662–6669; b) U. N. Fagioli, F. S. García Einschlag, C. J. Cobos, G. T. Ruiz, M. R. Féliz, E. Wolcan, *J. Phys. Chem. A* **2011**, *115*, 10979–10987.
[8] a) T. Biver, F. Secco, M. Venturini, *Coord. Chem. Rev.* **2008**, *252*, 1163–1177; b) G. T. Ruiz, M. P. Juliarena, R. O. Lezna, E. Wolcan, M. R. Feliz, G. Ferraudi, *Dalton Trans.* **2007**, 2020–2029.
[9] a) A. Vlček, in: *Photophysics of Organometallics*, vol. 29 (Ed.: A. J. Lees), Springer, Berlin/Heidelberg, **2010**, pp. 73–114; b) A. Kumar, S.-S. Sun, A. Lees, in: *Photophysics of Organometallics*, vol. 29 (Ed.: A. J. Lees), Springer Berlin/Heidelberg, **2010**, pp. 37–71.
[10] a) M.-W. Louie, T. T.-H. Fong, K. K.-W. Lo, *Inorg. Chem.* **2011**, *50*, 9465–9471; b) K. Lo, in: *Photophysics of Organometallics Vol. 29* (Ed.: A. J. Lees), Springer, Berlin/Heidelberg, **2010**, pp. 73–114.
[11] S. B. Jiménez-Pulido, M. Sieger, A. Knödler, O. Heilmann, M. Wanner, B. Schwederski, J. Fiedler, M. N. Moreno-Carretero, W. Kaim, *Inorg. Chim. Acta* **2001**, *325*, 65–72.
[12] a) O. Heilmann, F. M. Hornung, J. Fiedler, W. Kaim, *J. Organomet. Chem.* **1999**, *589*, 2–10; b) C. Bessenbacher, C. Vogler, W. Kaim, *Inorg. Chem.* **1989**, *28*, 4645–4648.
[13] a) T. Kojima, T. Sakamoto, Y. Matsuda, K. Ohkubo, S. Fukuzumi, *Angew. Chem.* **2003**, *115*, 5101; *Angew. Chem. Int. Ed.* **2003**, *42*, 4951–4954; b) C. Lorente, A. H. Thomas, *Acc. Chem. Res.* **2006**, *39*, 395–402.
[14] A. Odani, H. Masuda, K. Inukai, O. Yamauchi, *J. Am. Chem. Soc.* **1992**, *114*, 6294–6300.
[15] M. Mitsumi, J. Toyoda, K. Nakasuji, *Inorg. Chem.* **1995**, *34*, 3367–3370.
[16] a) B. Schwederski, W. Kaim, *Inorg. Chim. Acta* **1992**, *195*, 123–126; b) S. Miyazaki, T. Kojima, T. Sakamoto, T. Matsumoto, K. Ohkubo, S. Fukuzumi, *Inorg. Chem.* **2008**, *47*, 333–343; c) A. Abelleira, R. D. Galang, M. J. Clarke, *Inorg. Chem.* **1990**, *29*, 633–639.
[17] a) S. J. N. Burgmayer, E. I. Stiefel, *Inorg. Chem.* **1988**, *27*, 4059–4065; b) Y. Funahashi, Y. Hara, H. Masuda, O. Yamauchi, *Inorg. Chem.* **1997**, *36*, 3869–3875.
[18] J. Perkinson, S. Brodie, K. Yoon, K. Mosny, P. J. Carroll, T. V. Morgan, S. J. N. Burgmayer, *Inorg. Chem.* **1991**, *30*, 719–727.
[19] P. Basu, S. J. N. Burgmayer, *Coord. Chem. Rev.* **2011**, *255*, 1016–1038 and references therein.
[20] W. Kaim, B. Schwederski, O. Heilmann, F. M. Hornung, *Coord. Chem. Rev.* **1999**, *182*, 323–342.
[21] A. Crispini, D. Pucci, A. Bellusci, G. Barberio, M. La Deda, A. Cataldi, M. Ghedini, *Cryst. Growth Des.* **2005**, *5*, 1597–1601.
[22] a) W. Henderson, B. K. Nickleson, L. J. McCaffrey, *Polyhedron* **1998**, *17*, 4291–4313; b) T. C. John, *Int. J. Mass Spectrom.* **2000**, *200*, 387–401.
[23] G. Petroselli, M. K. Mandal, L. C. Chen, G. T. Ruiz, E. Wolcan, K. Hiraoka, H. Nonami, R. Erra-Balsells, *J. Mass Spectrom.* **2012**, *47*, 313–321.
[24] M. V. Werrett, D. Chartrand, J. D. Gale, G. S. Hanan, J. G. MacLellan, M. Massi, S. Muzzioli, P. Raiteri, B. W. Skelton, M. Silberstein, S. Stagni, *Inorg. Chem.* **2011**, *50*, 1229–1241.
[25] J. V. Caspar, T. J. Meyer, *J. Phys. Chem.* **1983**, *87*, 952–957.
[26] K. Hiraoka, K. Nishidate, K. Mori, D. Asakawa, S. Suzuki, *Rapid Commun. Mass Spectrom.* **2007**, *21*, 3139–3144.
[27] M. F. Wyatt, B. K. Stein, A. G. Brenton, *Anal. Chem.* **2005**, *78*, 199–206.
[28] C. K. Johnson, *ORTEP-II. A Fortran Thermal-Ellipsoid Plot Program*, Report ORNL-5318, Oak Ridge National Laboratory, Tennessee, USA, **1976**.
[29] A. Garrido Frenich, D. Picón Zamora, J. L. Martínez Vidal, M. Martínez Galera, *Anal. Chim. Acta* **2001**, *449*, 143–155.
[30] H. Lothar, *Coord. Chem. Rev.* **2008**, *252*, 2346–2361.
[31] R. Alberto, R. Schibli, R. Waibel, U. Abram, A. P. Schubiger, *Coord. Chem. Rev.* **1999**, *190–192*, 901–919.
[32] a) L. C. Chen, K. Nishidate, Y. Saito, K. Mori, D. Asakawa, S. Takeda, T. Kubota, H. Hori, K. Hiraoka, *J. Phys. Chem. B* **2008**, *112*, 11164–11170; b) L. C. Chen, K. Yoshimura, Z. Yu, R. Iwata, H. Ito, H. Suzuki, K. Mori, O. Ariyada, S. Takeda, T. Kubota, K. Hiraoka, *J. Mass Spectrom.* **2009**, *44*, 1469–1477.
[33] a) C. Hop, D. Saulys, D. Gaines, *J. Am. Soc. Mass Spectrom.* **1995**, *6*, 860–865; b) G. J. Van Berkel, S. A. McLuckey, G. L. Glish, *Anal. Chem.* **1992**, *64*, 1586–1593.

[34] H. Nonami, S. Fukui, R. Erra-Balsells, *J. Mass Spectrom.* **1997**, *32*, 287–296.
[35] *CrysAlisPro*, v. 1.171.33.48 (rel. 15–09–2009, CrysAlis171.NET), Oxford Diffraction Ltd..
[36] G. M. Sheldrick, *SHELXS-97, Program for Crystal Structure Resolution*, Univ. of Göttingen, Germany, **1997**.
[37] G. M. Sheldrick, *SHELXL-97, Program for Crystal Structures Analysis*, Univ. of Göttingen, Germany, **1997**.
[38] F. García Einschlag, *Kinesim*, v. 9.5, multipurpose program for kinetics and photochemistry (Copyright No. 395814), INIFTA, Argentina, **2005**..
[39] C. Ruckebusch, S. Aloise, L. Blanchet, J. P. Huvenne, G. Buntinx, *Chemom. Intell. Lab. Syst.* **2008**, *91*, 17–27.
[40] R. Tauler, *Chemom. Intell. Lab. Syst.* **1995**, *30*, 133–146.
[41] M. Goez, I. Sartorius, *J. Am. Chem. Soc.* **1993**, *115*, 11123–11133.
[42] M. Blanco, A. C. Peinado, J. Mas, *Anal. Chim. Acta* **2005**, *544*, 199–205.
[43] M. Meloun, J. Čapek, P. Mikšik, R. G. Brereton, *Anal. Chim. Acta* **2000**, *423*, 51–68.
[44] A. de Juan, R. Tauler, *Anal. Chim. Acta* **2003**, *500*, 195–210.
[45] P. Gemperline, E. Cash, *Anal. Chem.* **2003**, *75*, 4236–4243.
[46] M. Garrido, I. Lázaro, M. S. Larrechi, F. X. Rius, *Anal. Chim. Acta* **2004**, *515*, 65–73.

Received: June 21, 2012
Published Online: September 11, 2012

